Demonstration of Dipole-Induced Transparency Using Mirrored Split-Ring Resonator Metasurface For Microwave Applications

Sarin VP (sarincrema@gmail.com)
Government College Chittur
Rohith K. Raj
Govt. College manathavady
Vasudevan K
CUSAT: Cochin University of Science and Technology

Research Article

Keywords: Dipole induced transparency, metasurface, Spilt-Ring Resonators

Posted Date: January 10th, 2022

DOI: https://doi.org/10.21203/rs.3.rs-1222472/v1

Abstract

In this paper, dipole-induced transparency in the microwave regime is proposed and verified using experimental and simulation studies. A single layer mirrored Split-Ring Resonator (SRR) metasurface array working under the $H_{\perp}$ excitation scenario is used to achieveout-of-phase electric dipole moments on the metasurface for a normal incident plane wave. The emergence of the transparency window is accompanied by the destructive interference between out-of-phase oscillating electric dipole moments on the metasurfaceand is verified in computations by studying the radar Cross Section in full-wave electromagnetic simulations.We used the multipole scattering theory to validate the results computationally. The coupling effects are studied numerically, and the emergence of the transparency window is studied experimentally using transmission measurements inside an anechoic chamber using a vector network analyzer.

I. Introduction

Electromagnetically induced transparency (EIT) is a quantum interference effect occurring in atomic systems and is responsible for a transparency band within a broad absorption spectrum [1]. This transparency scheme modifies the dispersive nature of the opaque medium under consideration and shows electromagnetic wave slow down, resulting in enhanced light-matter interaction. EIT stems from the destructive interference or the dark superposition state from a multi-level system in which the net electric dipole moment of the atomic system is found to be vanished [2].Under the EIT conditions, the propagating electromagnetic wave experiences a large positive dispersion, and its group velocity will be significantly reduced [20]. This slow light effect is an essential characteristic of the EIT phenomenon and finds applications in quantum memories. When the light pulse enters an EIT medium, it gets slow down and undergoes spatial compression. The group velocity can be made zero by reducing the control field magnitude, causing the complete stopping of light and storing light within the medium.

EIT is also observed in classical coupled resonators in the optical domain and in resonator coupled optical waveguides [3–4]. Recently, metamaterials have been used to mimic EIT effects in the optical, THz, and microwave regimes [5–10]. The principle of metamaterial-induced transparency relies on the radiation interference between the “bright” and “dark” resonances excited on the composite. The bright resonator is typically superradiant and broad, which is efficiently coupled to the far-field. The external plane wave can directly excite this resonance, and its quality factor is very low.The dark resonance is a high Q resonance and is weakly coupled to free space. An asymmetry in the unit cell constituting the metamaterial creates anti-parallel currents or the magnetic resonance in the composite in which the created magnetic dipole moment will be parallel to the propagation direction. This mode shows strong confinement witha long lifetime and is a trapped mode [11–12]. The same trapped mode could be observed in identically stacked layers separated by a subwavelength distance, enabling strong anti-parallel currents on the plates resulting in destructive interference [13]. The sharp dispersion associated with the trapped mode resonance causes the electromagnetic pulse to be significantly delayed of the order 200 times that of the velocity in free space. Increasing the separation between the layers in these

double-layered structures causes a broader transparency resonance and a shorter lifetime. The Fano resonance-based EIT effects have been recently reported [14–15]. Fano resonances could also be excited in the visible regime from asymmetric plasmonic clusters [16–17] and could be used for achieving artificial magnetism at visible frequencies.

In this paper, we experimentally demonstrate the existence of Dipole Induced Transparency in the microwave regime using a mirrored array of SRR metasurface. The emergence of the transmission band within the forbidden energy gap is characterized by a dip in the Radar Cross Section of the composite. Multipole scattering theory reveals that the emergence of the transparency window is associated with scattering power suppression due to the resonant out-of-phase oscillation of electric dipole moments created on the composite. Experimental studies are performed inside an anechoic chamber using a vector network analyzer, and computations are performed using the full-wave electromagnetic simulation software CST Microwave Studio.

Ii. The Geometry Of The Problem

The fundamental constituent used in the study is the Split Ring Resonator (SRR). SRR unit cell is conventionally used to get the mu negative behavior at resonance as described by J.B Pendry [18]. The application of a plane wave with polarization parallel to the split with the incident magnetic field parallel to the axis of the SRR creates magnetic dipole moments parallel to the incident magnetic field. This excitation scenario is referred to as the $H_{||}$ excitation [19]. Another excitation is the $H_{\perp}$ scheme in which the incident electric field is parallel to the slits, the magnetic field is perpendicular to the axis of the SRR, and the direction of propagation is along the axis of the SRR element. This excitation creates strong electric dipole moments on the SRR array and these in-phase oscillating electric dipole moments create a dielectric bandgap.

We have used the $H_{\perp}$ excitation in this study, and the difference is that here the SRR array is not symmetrical. We have used a mirrored array of SRR to create a transparency window within the dielectric bandgap. The schematic of the proposed mirrored array of SRR is shown in Fig. 1. The SRR array is printed on an epoxy substrate having a relative dielectric constant of 3.8 and a height of 1.6 mm. The split gap is represented by ‘s’. The dimensions of the SRR are selected such that its resonant frequency lies within the microwave S-band. Parameter ‘g’ represents the offset between the line of symmetry indicated by the dotted lines and the SRR splits.

Iii. Results And Discussions

The Dipole Induced Transparency scheme using the proposed mirrored configuration is demonstrated in numerical simulations using the full-wave CST Microwave Studio software. The parameters of the proposed SRR array used for simulation studies are *r* = 6.7 mm, *d* = 2 mm, *s* = 0.8 mm, *w* = 1 mm and= 1.6 mm. The thickness of the metallic implant is 35μm. The periodicity of the SRR array is p= 20mm mm both in X and Y directions on both sides of the symmetry line. The displacement from the symmetry

line‘g_1’ is selected to be 1.1 mm. We have also simulated the single layer symmetric SRR array having the same dimensions for a comparison study. Here the periodicity of the array is selected to be 20 mm for the X and Y directions. Both the arrays use a total of 64 SRR elements in the plane.

For simulations, both the structures are illuminated with a plane wave traveling perpendicular to the plane of the SRR array with polarization along the Y-axis. We have studied the scattering characteristics of both these arrays using computation.

The Radar Cross Section (RCS) of a structure is defined as

$$\sigma = \lim_{R \to \infty} 4\pi R^2 \frac{|E_{sca}|^2}{|E_{inc}|^2}$$

1

Where R is the distance from the target to the observation point, E_{inc} is the incident electric field measured at the target's position, E_{sca} is the scattered electric field measured at the observation point. Fig. 2 shows the RCS of the symmetric and mirrored SRR arrays. As expected, the symmetric SRR array shows a hike in the scattering spectra at resonance centered on 2.28 GHz. This resonance is characterized by the dominant scattering contribution from the electric dipole (P_y) moments. The RCS value is significantly higher of the order of around 30425 mm^2 due to this bright electric dipole scattering and is said to be a highly visible resonance.

Interestingly, the RCS of the mirrored array shows low values indicated by the shadow region in comparison with the symmetric SRR array. This scattering reduction spans over a frequency range from 2.16 GHz to 2.26 GHz. This mirrored array is characterized by two resonant peaks separated by a scattering dip. The scattering dip is observed at 2.17 GHz, and correspondingly, the RCS value is found to be 16074 mm^2. The lower scattering hike is observed at 2.13 GHz with an RCS value of 18336 mm2. The second scattering peak occurs at 2.29 GHz with an RCS of 31634 mm^2. The mirrored array shows a slight blue shift in the scattering peak in comparison with the symmetric array and is more visible.

Measurements are performed inside an anechoic chamber using two Ultra Wide Band horn antennas. One horn antenna is configured in the transmission mode, and the other one is working in the reception mode. Initially, a THRU calibration is performed to nullify the path loss. The metasurface sample is inserted between these antennas such that the $H_{\perp}$ excitation scenario is achieved. The schematic of the measurement setup is shown in Fig. 3(a). The resulting transmission coefficients for the symmetric SRR array are illustrated in Fig. 3(b). As expected, the symmetric array shows a dielectric band gap centered around the resonant frequency f_s=2.28GHz, and correspondingly, the transmission coefficient is characterized by a dip showing resonant nature. The simulation and measurement are well matched. This resonance is characterized by strong electric dipole moments P_y and is caused due to the time-varying positive and negative charge distributions on the lower and upper unit cells. In the array, these electric dipole moments are oscillating in-phase, as shown in Fig. 3(c). The scattering characteristics of

this SRR array is also studied by exciting the entire array with an external plane wave with polarization along the Y-axis using CST Microwave Studio. At resonance, the structure shows symmetric forward and backward scattering,as shown in the inset of Fig. 3(b).

The symmetric array showing the bandgap is then replaced with the mirrored array configuration shown in Fig. 1. Fig. 4 illustrates the transmission characteristics of this array. It is evident from the graph that a resonant transparency window is created within the bandgap for the mirrored array. This transparency window is indicated using the shaded regions in the graph. Three resonant frequency points are observed designated as f_1, f_2, and f_3. The newly created resonant window is centered at f_2=2.21GHz. The transmission coefficient at this transparency window is found to be -0.6 dB in measurement.The transmission minima are found to be at f_1=2.13 GHz and f_3=2.32 GHz. The simulation and measurements are well matched.

The measured transmission phase of the two arrays is depicted in Fig. 4(b). The transmission phase shows distinctly different characteristics for the small frequency band under study. The symmetric SRR array shows smooth phase advancement across the bandgap. For the lower resonant dip around f_1, anomalous phase advancement is observed. Since the group delay is calculated as the negative rate of change of phase with frequency ($\tau = -d\Phi/d\omega$), this region is characterized by a negative group delay (GD). So this resonant dip can be said as a trapped mode, in which the electromagnetic energy is strongly confined within the vicinity of the metasurface. The transparency band centered on f_2 shows a sharp decrease in phase with respect to frequency. Correspondingly, the group delay will be positive, causing a significant delay for the transmitted pulse. The reflection resonance at f_3 is characterized by an abrupt phase jump characterizing a reflective resonance.

Simulation studies are also performed to find out the nature of electromagnetic power flow across the dispersion band under consideration. Fig. 5 shows the Poynting vector distributions of the mirrored array for the three frequency points. The plane wave is travelling aling the Z-axis from top to the bottom of the computational domain. It is obvious that for the trapped mode resonance centered around 2.16 GHz (Fig. 5.(a)), a transverse flow of electromagnetic power is observed at the discontinuous boundary of the metasurface layer. The circulation of Poynting vecot distribution near the metasurface boundary confirms the presence of the trapped mode. At this trapped mode resonance, the electromagnetic waves experience a large life time enabling maximum light-matter interaction. For the transparency window centered sround 2.21 GHz(Fig. 5.(b)), the pointing vector distributions are normal to the entrance and exit faces indicating a smooth electromagnetic power flow across the boundary. At this transparency window, the structure shows minimum scattering and is responsible for the RCS dip. This smooth flow of electromagnetic power is similar to that observed in electromagnetic cloaking schemes [20]. The highly reflective resonance shown in Fig. 5.(a) around 2.32 GHz, shows a significant perturbation of electromagnetic power flow and shows a high RCS value. It is noted that for the three frequency points edge diffraction is observed on the left and right boundaries of the metasurface.

The scattering behavior of the mirrored array depicted in Fig. 2(a) shows a close similarity with a Fano resonance profile [21]. In Fano resonance, the destructive interference is achieved by the combined effect of electric and magnetic resonance to reduce total scattering and shows asymmetric scattering profile. But, here the situation is quite different. To understand the exact reason behind these peculiar scattering characteristics, we used the multipole scattering theory. Since the $H_{\perp}$ excitation scheme induces only the electric dipole moment on the SRR composite; only the power scattered from the electric dipole moment is expected. The induced dipole moments could be calculated by spatial integrating the surface current density excited on the composite as [22]

$$\mathrm{P} = \frac{1}{\mathrm{i}\omega}\int \mathrm{J}\mathrm{d}^3\mathrm{r}(2)$$

$$M = \frac{1}{2c}\int \left(\vec{r}XJ\right)d^3r\left(3\right)$$

$$T = \frac{1}{10c}\int [(\vec{r}.J) - 2r^2J]d^3r(4)$$

Where P,M, Trepresent the induced electric, magnetic, and Toroidal dipole moments, ω is the angular frequency, J is the volume current density, r is the distance to the far-field observation point.

The normalized scattered power from these dipole moments with respect to the symmetric SRR array is shown in Fig. 6. It is noted that the power radiated from the electric and toroidal dipole moments shows a dip around the transparency window. For the entire transparency window, the radiated power from the electric dipole moment is lesser than the symmetric SRR array. It is to be noted that the power radiated from the toroidal moment for the mirrored array is in comparison with that for the mirrored array. Moreover, the electric dipole moment's radiated power is tremendously higher than that from the toroidal moment for the mirrored array. The magnetic dipole moment is non-resonant because the $H_{\perp}$ excitation scenario is incapable of exciting resonant magnetic dipole on the composite. The orientation of the magnetic dipole moment is directed along the direction of propagation (Z-axis), and hence it is weekly coupled to free space. Hence it can be concluded that the transparency window emerges due to the cancellation of radiated power from the electric dipole moment.

This scattering cancellation effect can be well understood by studying the phase of electric field distributions (E_y) taken over the two arrays,as shown in Fig. 7. It is observed that for the symmetric array indicated by the solid black lines, the phase of the electric field across the array remains almost steady. It means that the electric dipole moments are oscillating in-phase resulting in a bandgap. But for the mirrored array, the distributions show phase alterations around the symmetry line as indicated by the black dashed lines. It is observed that the mirror SRR lying near the symmetry line are excited in-phase, whereas the distant ones are oscillating out-of-phase with respect to the center ones. These out-of-phase oscillations between the electric dipole moments cancel the far-field scattered power resulting in the emergence of the transparency window.

Parametric analysis has been performed to find out the effect of various parameters on scattering spectra. Fig. 8(a) shows the effect of the gap parameter ‘g’ on the scattering spectrum. For all these variations, a normal incidence plane wave is considered. It is observed that the scattering dip will be more pronounced when the mirrored elements are brought closer to each other. As ‘g’ is increased, a redshift in the scattering maximum is observed. When ‘g’ is increased above 3.1mm, no significant change in the scattering dip is observed. Parametric studies have also been performed by varying the angle of incidence along the azimuth plane, and these results are shown in Fig. 8(b). It is noted that the angle of incidence plays a crucial role on the scattering dip. The scattering dip around 2.17 GHz is clearly observed for normal incidence. As the angle of incidence increases in steps of 10^0, the structure loses the scattering reduction behavior. When the incident angle is increased beyond 20^0, the scattering behavior looks similar to the symmetric SRR array, and the transparency window is found to have vanished.

Iv. Conclusion

In this paper, an experimental and computational demonstration of Dipole Induced Transparency scheme in the microwave regime is presented. Multipole scattering theory has been utilized to find the exact reason behind the emergence of this transparency window. The mirror symmetry in the orientation of the SRR array creates an out-of-phase oscillation of electric dipole moments, resulting in scattering suppression from the composite at the far-field. This scattering cancellation scheme is computationally verified using full-wave simulations and found that the transparency window is associated with a dip in the Radar Cross Section of the composite. Parametric studies have also been performed to find out the effect of various parameters on scattering characteristics.

Declarations

Acknowledgment

The authors acknowledge the research funding received from the Science and Engineering Research Board (SERB), Department of Science and Technology, for the major research project ECR/2017/002204.

Conflicts of Interest

There are no conflicts of interest

References

1. Xu, Q., Sandhu, S., Povinelli, M.L., Shakya, J., Fan, S., Lipson, M.: “Experimental realization of an on-chip all-optical analogue to electromagnetically induced transparency,” Phys. Rev. Lett., vol. 96, no. 12, 2006

2. M. Fleischhauer, A. Imamoglu, and J. P. Marangos, “Electromagnetically induced transparency: Optics in coherent media ”, Rev. Mod. Phys. 77, 633, 2005
3. Bajcsy, M., Zibrov, A.S., Lukin, M.D.: Stationary pulses of light in an atomic medium. Nature. **426**(6967), 638–641 (2003)
4. Waks, E., Vuckovic, J.: “Dipole induced transparency in drop-filter cavity-waveguide systems,” Phys. Rev. Lett., vol. 86, no. 15, 2006
5. Dong, Z.-G., Liu, H., Cao, J.-X., Li, T., Wang, S.-M., Zhu, S.-N., Zhang, X.: “Enhanced sensing performance by the plasmonic analog of electromagnetically induced transparency in active metamaterials,” Appl. Phys. Lett., vol. 97, no. 11, 2010
6. Chakrabarti, S., Ramakrishna, S.A., Wanare, H.: “Coherently controlling etamaterials,” Opt. Exp., vol. 16, no. 24, pp. 19 504–19 511, 2008
7. Liu, N., Langguth, L., Weiss, T., Kastel, J., Fleischhauer, M., Pfau, T., Giessen, H.: Plasmonic analogue of electromagnetically induced transparency at the Drude damping limit. Nature Mater. **8**(9), 758–762 (2009)
8. Kim, J., Soref, R., Buchwald, W.R.: Multi-peak electromagnetically induced ransparency (EIT)-like transmission from bull’s-eye shaped metamaterial. Opt. Lett. **19**(17), pp. 17 997–918 002 (2010)
9. Chiam, S.-Y., Singh, R., Rockstuhl, C., Lederer, F., Zhang, W., Bettiol, A.A.: “Analogue of electromagnetically induced transparency in a terahertz metamaterial,” Phys. Rev. B, Condens. Matter, vol. 80, no. 15, 2009
10. Meng, F.-Y., Zhang, F., Zhang, K., Wu, Q., Kim, J.-Y., Choi, J.-J., Lee, B., Lee, J.-C.: Low-loss magnetic metamaterial based on analog of electromagnetically induced transparency. IEEE Trans. Magn. **47**(10), 3347–3350 (2011)
11. Fedotov, V.A.: M. Rose, Prosvirnin, S.L. N. Papasimakis, *and* Zheludev, N.I. “Sharp Trapped-Mode Resonances in Planar Metamaterials with a Broken Structural Symmetry”,Phys. Rev. Lett. 99, 147401, 2007
12. Chiam, S.-Y., Singh, R., Rockstuhl, C., Lederer, F., Zhang, W., Bettiol, A.A.: Analogue of electromagnetically induced transparency in a terahertz metamaterial. Phys. Rev. B **80**, 153103 (2009)
13. Papasimakis, N., Fedotov, V.A., Zheludev, N.I., Prosvirnin, S.L.: Metamaterial Analog of Electromagnetically Induced Transparency. Phys. Rev. Lett. **101**, 253903 (2008)
14. Song Han, R., Singh, L., Cong, Yang, H.: Engineering the fano resonance and electromagnetically induced transparency in near-field coupled bright and dark metamaterial. J. Phys. D: Appl. Phys. **48**, 035104 (2015)
15. Papasimakis, N.: NI Zheludev”Metamaterial-induced transparency: Sharp Fano resonances and slow light”. Optics and Photonics News **20**(10), 22–27 (2007)
16. Shafiei, F., Monticone, F., Le, K.Q., Liu, X.X., Hartsfield, T., Alù, A., Li, X.: A subwavelength plasmonic metamolecule exhibiting magnetic-based optical Fano resonance. Nature nanotechnology **8**(2), 95–99 (2013)

17. Ben Hopkins, Dmitry, S., Filonov, A.E., Miroshnichenko, F., Monticone, A., Alu, Y.S., Kivshar: Interplay of magnetic responses in all-dielectric oligomers to realize magnetic Fano resonances. Acs Photonics **2**(6), 724–729 (2015)
18. Pendry, J.B., Holden, A.J., Robbins, D.J., Stewart, W.J.: ” Magnetism from conductors and enhanced nonlinear phenomena”. IEEE Trans. Microwave Theory Tech. **47**(11), 2075–2084 (1999)
19. Smith, D.R., Padilla, W.J., Vier, D.C., Nemat-Nasser, S.C., Schultz, S.: Composite Medium with Simultaneously Negative Permeability and Permittivity. Phys. Rev. Lett. **84**, 4184 (2000)
20. Alù, A., Engheta, N.: Cloaking a sensor. Phys. Rev. Lett. **102**, 233901 (2009)
21. Shafiei, F., Monticone, F., Le, K.Q., Liu, X.X., Hartsfield, T., Alù, A., Li, X.: A subwavelength plasmonic metamolecule exhibiting magnetic-based optical Fano resonance. Nature nanotechnology **8**(2), 95–99 (2013)
22. Papasimakis, N., Fedotov, V.A., Savinov, V., Raybould, T.A., Zheludev, N.I.: Electromagnetic toroidal excitations in matter and free space. Nat. Mater. **15**(3), 263–271 (2016)

Figures

Figure 1

Geometry of the Mirrored SRR array

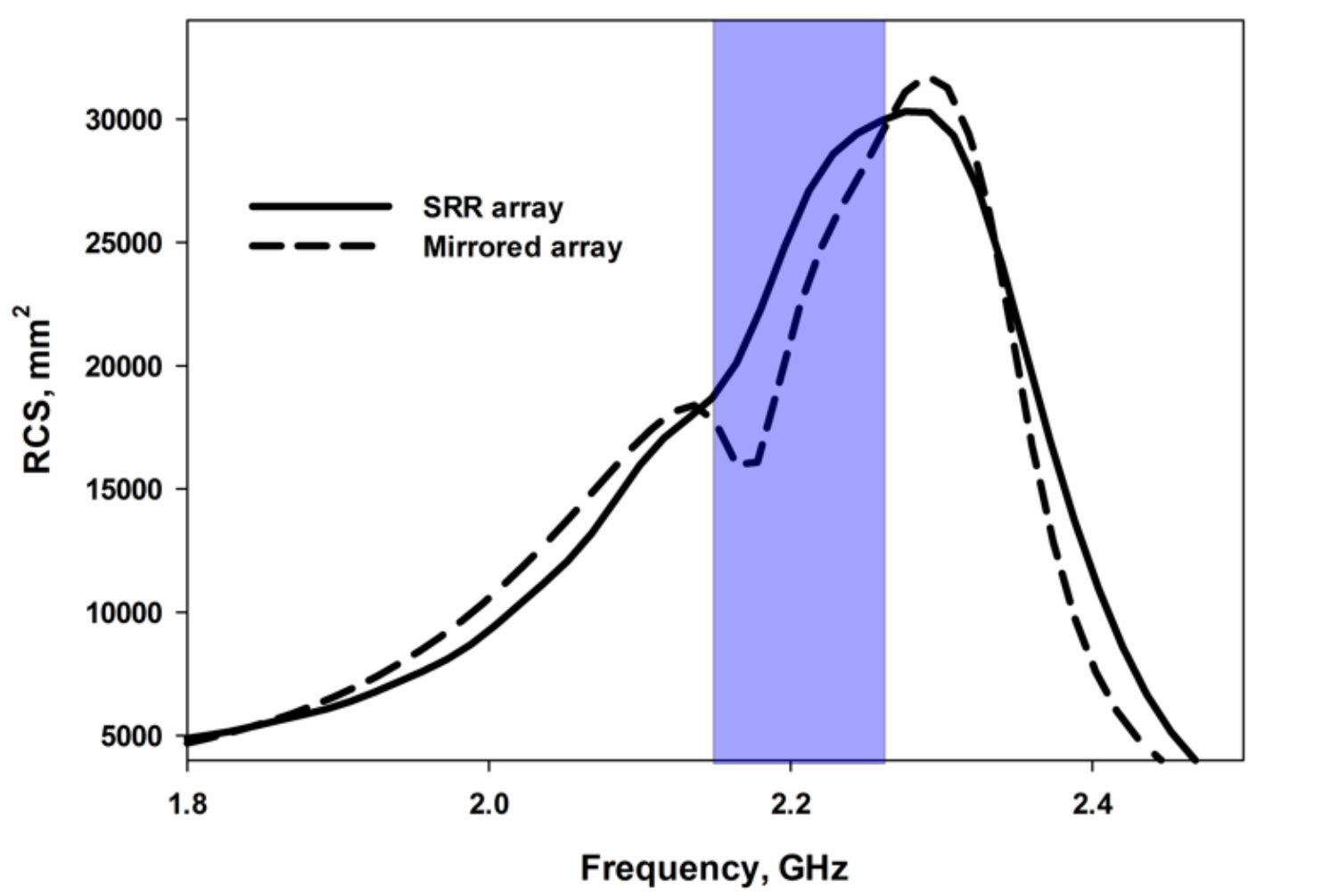

Figure 2

RCS of the symmetric SRR array (Solid line) and the Mirrored array (dashed line)

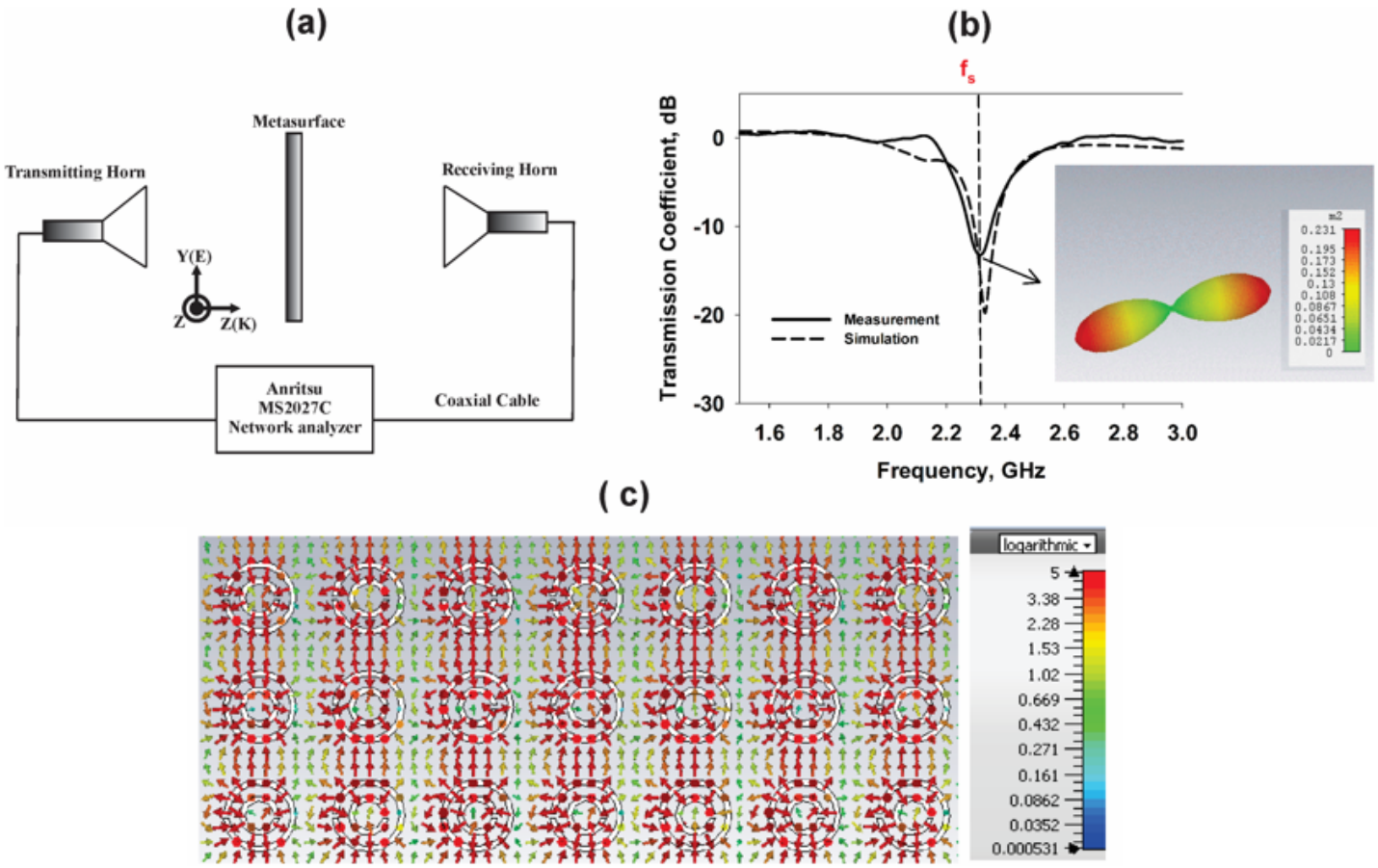

Figure 3

a) Measurement setup for characterizing the metasurface, b) Simulated and measured transmission Coefficients of the SRR array, c) Electric field distribution at resonance (2.28 GHz)

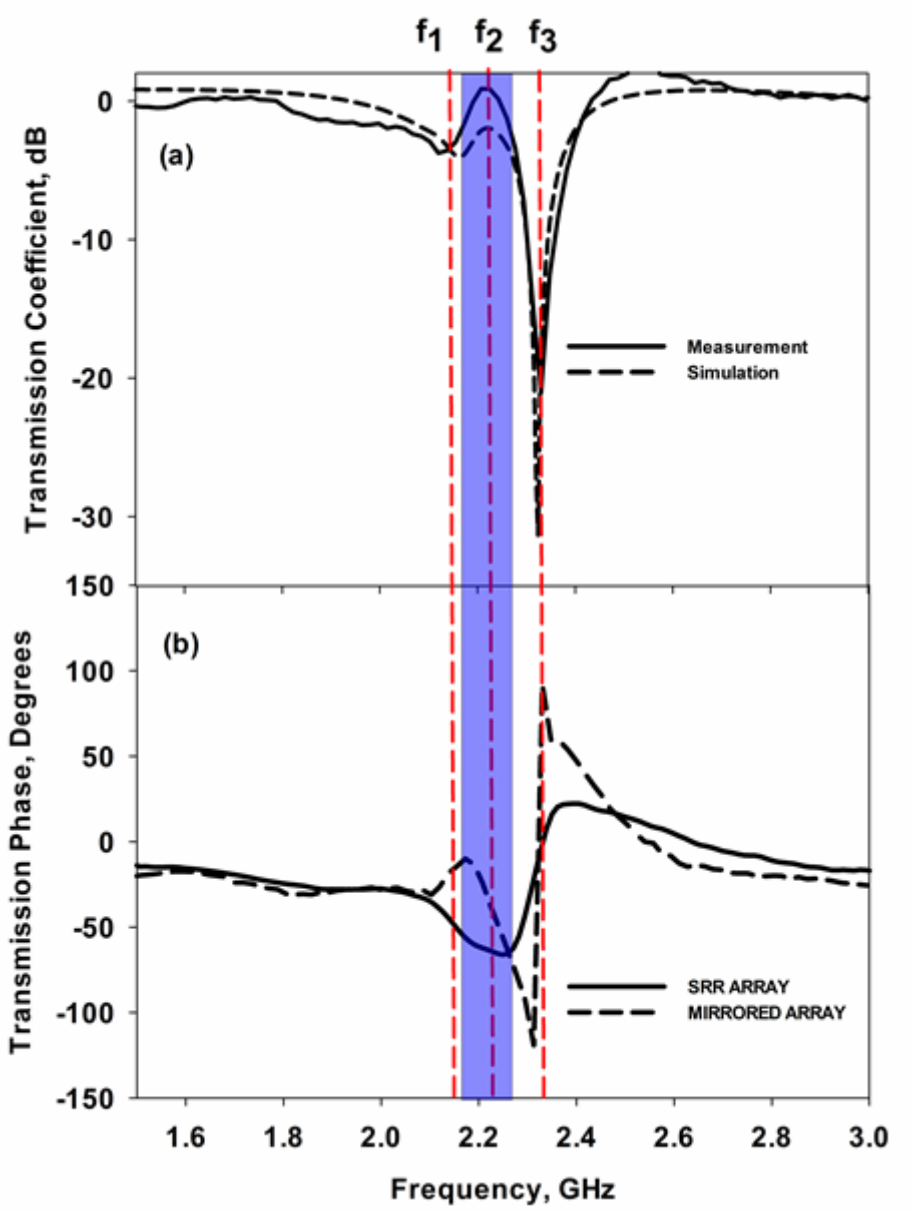

Figure 4

a) Simulated and measured transmission coefficients of the mirrored SRR array, b) Measured transmission phase of the mirrored and SRR arrays

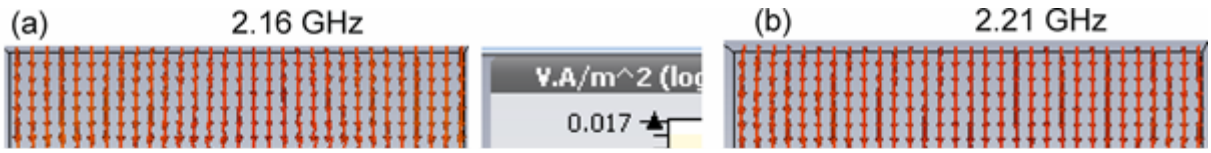

Figure 5

Simulated Poynting vector distributions a) at 2.16 GHz, b) 2.21 GHz and c) 2.32 GHz

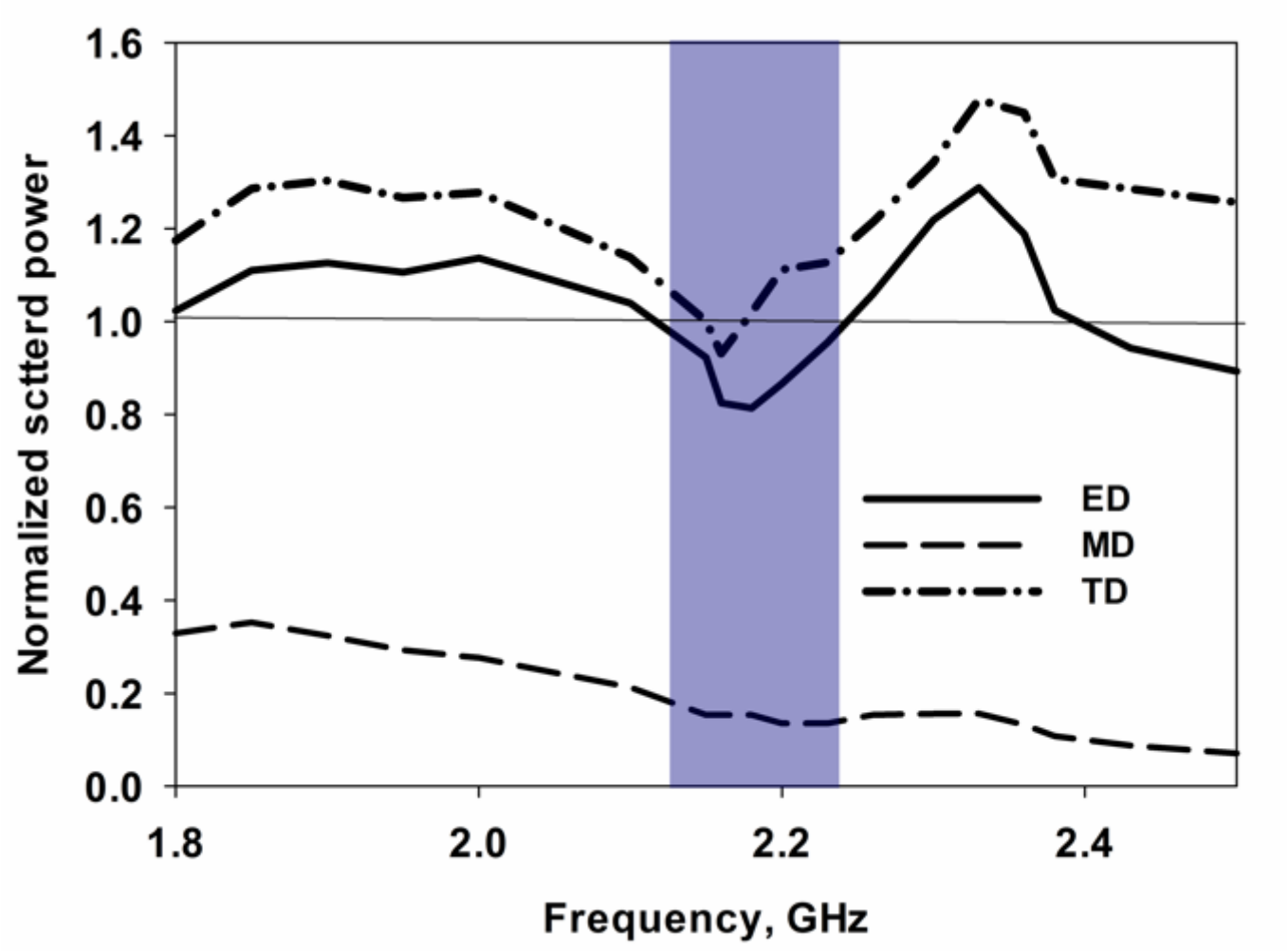

Figure 6

Normalized scattered power from different multipoles

Figure 7

Phase variation of electric field (Ey) distributions just above the two arrays

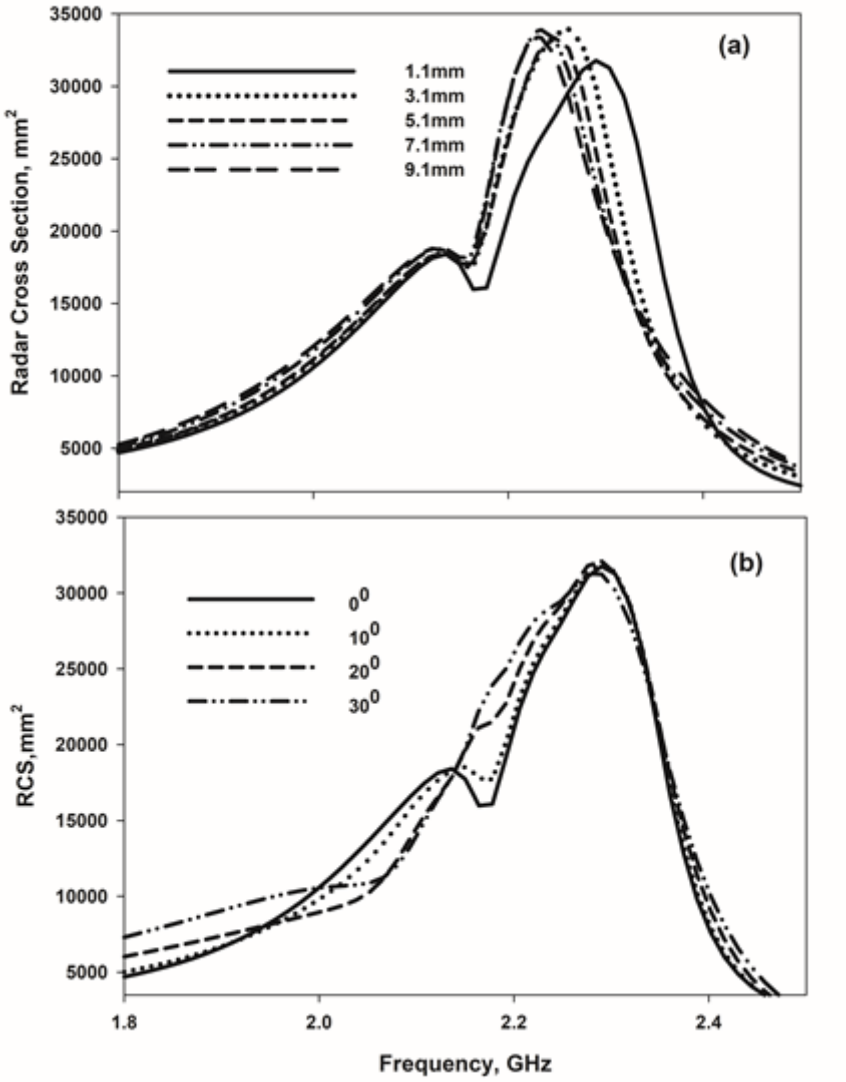

Figure 8

Parametric variation studies a) Effect of gap parameter ‘g’ and b) effect of angle of incidence in the azimuth plane on scattering characteristics